10IKC-44

METASOMATISM IN CRATONIC MANTLE ROOT: INSIGHT FROM GEOCHEMISTRY OF DEFORMED PERIDOTITE XENOLITHS OF UDACHNAYA PIPE

Agashev A M [1]*, Ionov D A[2], Pokhilenko N P[1], Golovin A V[1], Surgutanova E A [1], Sharygin I S.[1]

[1]Inst. Geology & Mineralogy, Novosibirsk 630090, Russia (* correspondence: agashev@igm.nsc.ru)
[2]Université J. Monnet, Saint-Etienne 42023, France

Introduction

Peridotites of cratonic mantle (CM) are represented by two texturally distinct types: coarse (granular) peridotites and deformed (sheared) peridotites. In contrast to the granular type, deformed peridotites display a bimodal grain size with large porphyroclasts residing in fine-grained neoblast matrix. Pressure and temperature (P-T) estimates of mineral equilibration of peridotites make up a conductive type of geotherm, however deformed peridotites usually yield higher P-T estimates and define an inflection to a convective geotherm. Presently, deformed peridotites are considered as refertilized parts of Archean CM (O'Reilly and Griffin, 2010 and references therein) which compose the lower layer of CM. While the origin of deformed peridotites remains controversial, interaction with convecting asthenosphere is generally considered as the main explanation of their textures and composition. Recent publications consider the formation of deformed peridotites to be linked to crystallization of megacryst suites (Burgess and Harte, 2004; Solov'eva et al, 2008) and kimberlite melt formation (Agashev et al, 2010) within a single event of thermal perturbation at the CM base. In recent years, unique fresh mantle xenoliths have became available from kimberlite pipe Udachnaya located in the Siberian platform within the Daldyn kimberlite field. The present study is devoted exclusively to deformed peridotites based on a representative collection of some 22 fresh and large deformed peridotite xenoliths from the eastern body of the Udachnaya pipe. Samples were studied for the chemical composition of WR and their constituent minerals with the purpose to clarify the composition and geochemical evolution of CM base.

Petrography

All samples are typical four phase peridotites, consisting of variable amounts of olivine (Ol), orthopyroxene (Opx), clinopyroxene (Cpx) and garnet (Gar). Seven samples could be classified as garnet-harzburgites as they have less than 5% of modal Cpx in their mineralogy. The others are garnet-lherzolites. The xenoliths have a porphyroclastic or mosaic-porphyroclastic textures (Harte 1977) composed by bigger grains of major phases that setting in matrix of fine-grained sugar-like olivine neoblasts. The degree of deformation show by samples is significantly variable as well as neoblasts to porphyroclasts ratios and their grain sizes. The rocks represent a sequence of transition from initial stages of deformation with relicts of granular textures (Uv-24/05) to strongly deformed fluidal textured specimens with minerals elongated and oriented into the chains and layers (Uv 3/01) (Figure 1). The grain size of porphyroclasts minerals are ranging from the 1-2 mm and up to 12mm in different samples.

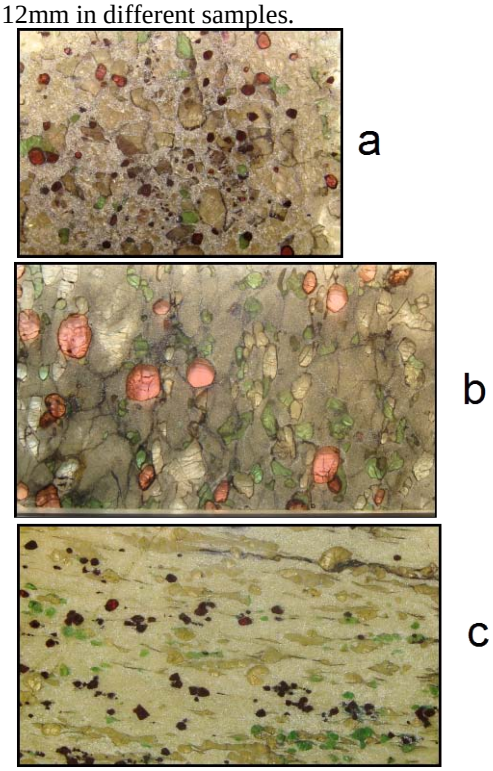

Figure 1. Textural variations in deformed peridotite xenoliths from kimberlite pipe Udachnaya. a) sample Uv-252/02 with low deformation degree. b) medium-deformed sample Uv 268/02. c) Sample Uv 3/01 displays the highest deformation with broken garnets arranged as linear chains. View field is 3cm along the long axis for a) and 4 cm for other samples.

Mineral chemistry

Olivine Mg# *[Mg/(Mg+Fe)$_{at}$]* ranges from 86.4 to 91.3; it correlates positively with concentrations of NiO. The compositions of olivine porphyroclasts and neoblasts are practically identical within a particular sample. Olivine Mg# define two distinct groups with Mg# 89.4-91.7 and 86.4-87.5. Orthopyroxene from deformed peridotites have Mg# (88.2–92.9) that are slightly higher than in olivines and positively correlate with Mg# of olivines. The sharp compositional discontinuity is also evident in the Opx's, clearly dividing Fe enriched group from the rest of samples.

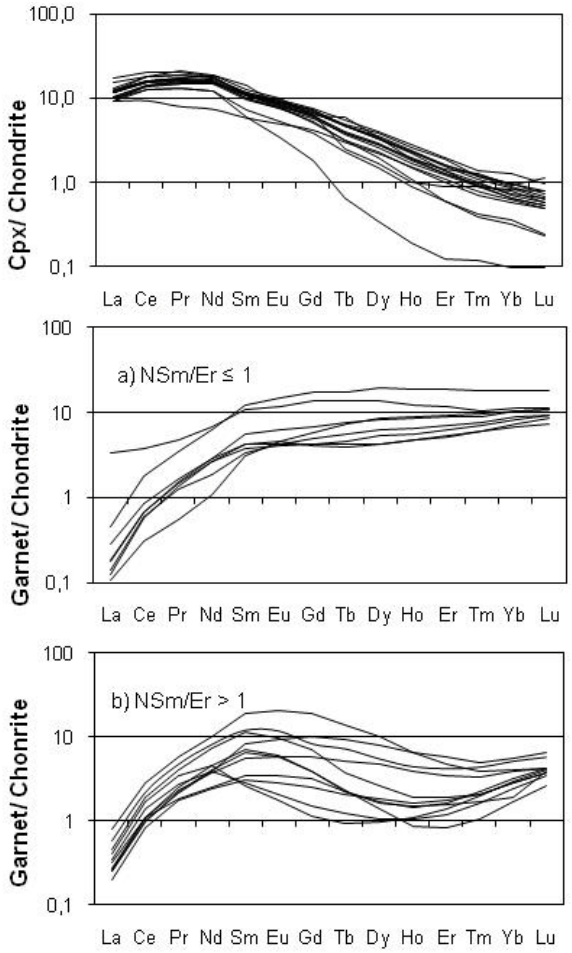

Figure 4. Chondrite-normalized REE patterns of clinopyroxenes and garnets of deformed peridotite xenoliths from Udachnaya pipe.

Clinopyroxenes from deformed peridotites are low in CaO, with 35.9–43.3 mol %. of diopside component, Ca/(Ca + Mg), indicating high equilibration temperatures. REE patterns of the cpx are enriched in LREE with a maxima at Ce-Nd, which is typical for cpx of deformed peridotites (Pearson et al, 2003). The shape of these patterns is uniform for the vast majority of samples (Fig 2.). The chemical composition of garnets from deformed peridotites shows great variability in their Cr_2O_3 contents (1.8-12.2 Wt%). Most of the garnets composition are in agreement with metasomatic evolution trend of type I (Burgess and Harte 2004), with decrease of CaO and Cr_2O_3 contents along the lherzolite trend. Low Cr garnets composition is approaching that of megacryst garnets from Udachnaya kimberlite reported in Agashev et al (2006). Garnets can be divided in two groups based on the shape of their REE patterns. First group have a sinusoidal REE pattern which is a usual feature of harzburgitic (low CaO) garnets included in diamonds (Stachel 2008). The second group has a flat REE pattern from MREE to HREE, and a sharp decrease from Nd to La, which is common for garnet megacrysts and high-T lherzolites (Burgess and Harte 2004). Calculated value Sm_n/Er_n (n-normalized to chondrite) which can be used as a measure of pattern sigmodality are <1 in the first group and >1 in the second, and positively correlates with Cr_2O_3 in garnets.

Whole Rock Chemistry

All the samples are enriched in MgO compared to the primitive mantle (PM) composition of McDonough and Sun (1995) and have a wide variation in their MgO contents (38,5 – 46 Wt%), but have a little variation in amount of SiO_2 (42.3-44.7).

The deformed peridotites are depleted in magmaphile elements (CaO, TiO_2 and Al_2O_3) comparative to PM that indicate their residual nature. FeO and K_2O behave independently from other elements in deformed peridotite compositions. Concentrations of FeO are scattered around the PM value and four samples are significantly enriched in FeO (10,7-12,1 Wt %). Amount of K_2O in all samples of deformed peridotites are significantly higher than that of PM reaching up to 0,25 wt% and in average higher than amount of Na_2O. FeO and K_2O concentrations in deformed peridotites do not correlate between each other, but FeO correlates with TiO_2 , and K_2O shows rough correlation with CaO. The later indicates that enrichment of deformed peridotites in FeO and K_2O result from different processes. Most of the peridotite samples have a negative loss of ignition (LOI) with indicates weight increase during heating and oxidation of FeO to Fe_2O_3 ; this supports visual observations of exceptional freshness of the samples. Only two samples could be considered as slightly altered as their LOI values are 0,57-0,98 wt%.

The deformed peridotites are enriched in the highly incompatible elements with bulk Kd (mineral/melt distribution coefficient) <0,01. The degree of enrichment in particular elements ranges from 2-10 times PM abundances for K and Rb to 1-5 times PM for Ba, Th, U, Nb and La. The concentration of elements of middle incompatibility (MREE, Zr, and Hf) varies around PM model composition

and even slightly depleted in most of the samples. Heavy REE and Y concentrations are lower than that of PM model. The patterns (Fig. 3) have positive peaks at Rb, K and Ti and minimum at Th. The shape of these patterns differs from that of host kimberlite.

Concentrations of highly incompatible elements well correlate between each other and with concentrations of P_2O_5 and do not correlate with LILE (Rb, Ba, K) abundances. Concentrations of elements of middle incompatibility to peridotite mineralogy (Zr, Hf and MREE) well correlate with TiO_2, CaO and Na_2O. HREE abundances show good correlations with those of Al_2O_3 and CaO.

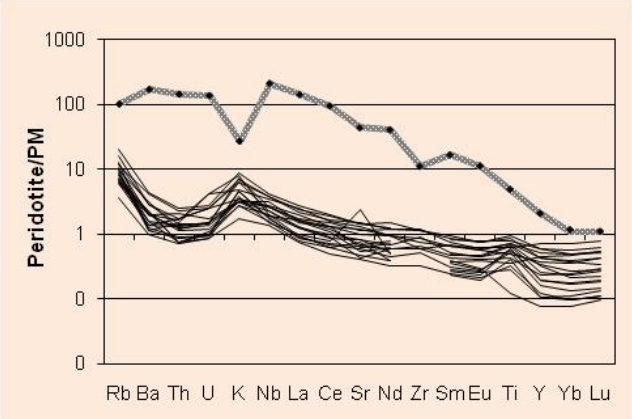

Figure 3. PM-normalized trace elements patterns of deformed peridotites and their host kimberlite (upper line).

Mantle metasomatism

It has been generally accepted in recent years that CM peridotites are formed as high-degree melt extraction residues either by shallow melting at the spinel stability field and subsequent subduction or deeply by plume subcretion. All hypotheses consider that all Cpx and probably all of Gar (Simon et al, 2007 and references therein) are later metasomatic products in ultradepleted peridotites originally composed of Ol+Opx. However, details of metasomatic processes, sequence of mineral precipitation and the nature of metasomatic agents are a matter of debate.

Deformed peridotites of Udachnaya contain widely variable modal Cpx and Car ; and amount of both minerals correlates with CaO and Al_2O_3 in the WR. Temporal relations between Cpx and Garnet could be evaluated from their geochemistry. Garnets of our deformed peridotites are subdivided into two subsets based on their REE pattern, sinusoidal with $Sm_n/Er_n > 1$ and normal with $Sm_n/Er_n \leq 1$. In two of our samples, both FeO-rich, garnets are zoned with REE patterns sinusoidal in cores and normal at the rims. The latter could be evidence for two garnet generations within the rocks, probably from different metasomatic agents. In contrast to Gar, clinopyroxenes of Udachnaya deformed peridotites have uniform (except two samples) REE patterns. The Cpx's are not in trace element equilibrium with garnets of $Sm_n/Er_n > 1$ group, indicating that Cpx's crystallized later, together with normal garnet.

HREE-depleted garnets could be an early metasomatic phase in mantle peridotites and, as proposed in (Pearson et al, 1995; Simon et al, 2007), were formed at the expense of Opx by reaction with metasomatic fluid. In our samples, these originally cubcalcic garnets experienced an influence of later silicate metasomatism and became lherzolitic in terms of major elements, but retain the sinusoidal REE pattern, similar to garnets of lherzolitic paragenesis included in diamonds Stachel (2008). Burgess and Harte (2004) explained the variability of peridotitic garnet REE patterns by percolative fractionations of metasomatic melt during its ascent though peridotites. Normal REE patterns of the garnets at the bottom of CM are gradually changed to sinusoidal in the middle of CM section according to changes in fractionating liquid composition, from which garnets were crystallized. In our sample suite there is no correlation between P estimates and Sm_n/Er_n ratios and therefore no correlation of garnet REE patterns with depth of their formation. Since, we suppose that difference in REE patterns of garnets are rather a function of distance from veins of asthenospheric melt then the distance of vertical travel of this melt. The final REE pattern of garnets depends on degree of metasomatic melt fractionation, volume of melt arrived at certain point, degree of equilibrium and the number of metasomatic pulses.

All discussion in this chapter mostly concerns modal metasomatism, however WR are enriched in highly incompatible elements which could be related to cryptic metasomatism. High concentrations of these elements are attributed to submicron-size metasomatic phases located along the grain boundaries of rock-forming minerals. Although, the exact residence of these elements is not a purpose of present study, Sharygin et al (2011, in press) detected following submicron phases in deformed peridotites: apatite, phlogophite, spinel+magnetite, perovskite, sulphides and carbonates, partly in the same samples that used in this study. Concentrations of very incompatible elements well correlate with P_2O_5 and therefore main hosts of these elements (except K, Rb and Ba) should be apatite and carbonates.

Nature of metasomatic agent

Evidence from mass-balance calculations

To evaluate the nature of the metasomatic agent we compare calculated and measured WR rock trace element compositions. In calculations of WR composition, modal mineralogy and composition of Gar and Cpx were used.

Comparison displays large difference between calculated and measured WR trace element composition, and concentrations of incompatible elements in calculated data are always lower than that of measured. The most pronounced differences are observed for highly incompatible elements (Nb, Ta, Th, U, Rb and Ba), and their concentrations in the calculated composition never exceed 20% of the measured WR composition. Significant amounts of La and Ce are incorporated into Cpx, and calculated WR composition mostly contains 20-40% of these elements budget. The middle REE in calculated WR composition comprise from 60 to 100% of the rock budget as they enter both Cpx and Gar. Most of HREE also incorporated into Cpx and Gar (50-90% of the rock budget) and nearly half of the samples have similar calculated and measured composition in terms of MREE concentrations.

Schmidberger and Francis (2001) explained discrepancies between measured and calculated WR compositions by infiltration of 0.4-2% of host kimberlite into the rock. Our modeling shows that the REE contents of only four samples could be closely reproduced by addition of kimberlite melt to the calculated WR composition (Fig. 4).

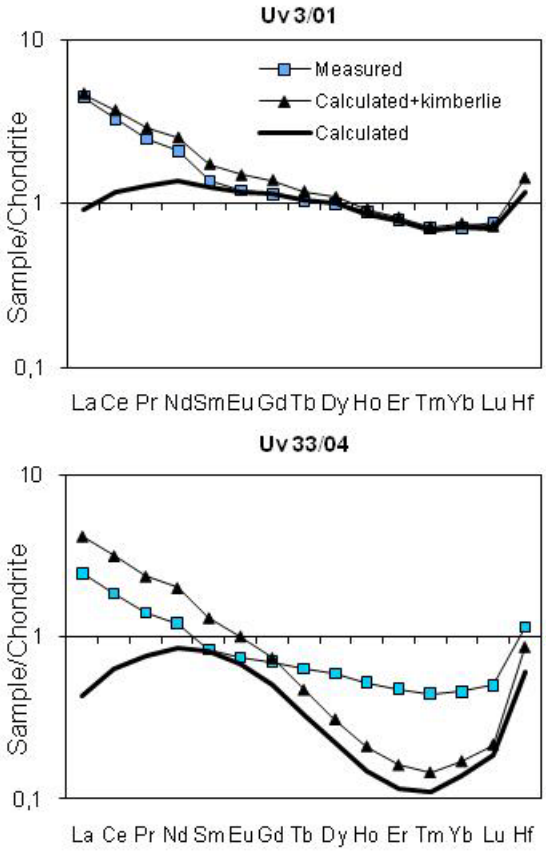

Most of the samples require a metasomatic agent with a much lower La/Yb ratio and LREE abundances than kimberlites; therefore we try to search for a candidate of such an agent among incompatible element-enriched OIB. The HIMU type basalts of St. Helena islands (Willbold and Stracke, 2006) are enriched in incompatible elements, and calculation shows that they could be an appropriate metasomatic agents. However, in most cases, the discrepancies are observed in the MREE contents, as abundances of these elements in modeled compositions are higher than in measured. This feature could be a consequence of preferred incorporation of MREE into Cpx and Gar from infiltrating melt.

Another way to evaluate the fingerprints of metasomatic agent is to look at the ratios between elements of similar geochemical behavior. In our case the elements which do not enter into modal mineralogy and therefore do not fractionate against each other could provide most useful information about geochemical signatures of metasomatic agent. The ratios between Nb, Th, U, La and Rb can be used as an example. Most of the measured WR have Th/U ratios similar to HIMU basalts and little lower than in host kimberlite, but their Nb/La ratios are more similar to kimberlite although it intersects with HIMU OIB. Both discussed ratios in calculated WR composition are lower than in measured indicating preferred incorporation of La and U into Cpx from infiltrating melt. Ratios between Nb and Th are similar in all discussed substances indicate that those elements do not fractionate against each other during metasomatic processes in the mantle. In contrast, Rb/Nb ratios in measured WR are much higher than that in calculated and in the kimberlites and HIMU basalts. This feature is explained by preferred incorporation of LILE into kelyphitic rims around garnet grains which disturbs the original Rb/Nb ratio of metasomatic agent.

Conclusions

We can conclude that at least 4 different types of metasomatic enrichment are evident in chemical composition of deformed peridotite xenoliths. It are hydrous or carbonatitic fluid, silicate, Fe-rich and K metasomatose. The temporal relation between types of metasomatic enrichment is not very clear, but fluid metasomatoism was the fist and Fe-enrichment could be the latest.

Metasomatic evolution of rocks at the base of the lithospheric mantle is started by introduction of low amounts of melts/fluids rich in incompatible elements, probably of carbonatitic composition. Metasomatism at this stage was mostly cryptic; however it leads to formation of subcalcic high Cr garnets with sinusoidal REE pattern, probably at the expense of Opx. This process led to a small increase of Al and Ca contents in WR of originally

ultradepleted peridotites and it significantly increases their La/Yb ratio.

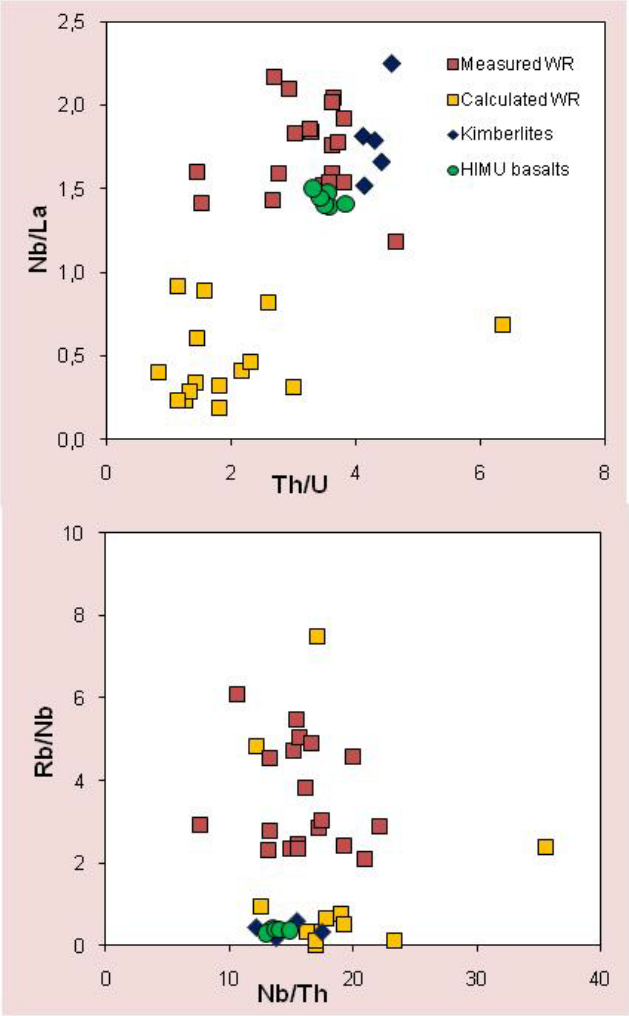

Figure 5. Ratios between very incompatible elements in measured and calculated WR compositions of deformed peridotites compared to these ratios in HIMU basalts and kimberlite melts

The next stage of metasomatic enrichment is the most important for peridotites as we see them today and led to significant changes in modal mineralogy of deformed peridotites. This stage of metasomatism could be induced via introduction of astenoshperic melt of enriched OIB (HIMU) affinity which could evolve through the fractional crystallization to composition close to kimberlitic. Introduction of this melt and its reaction with initially depleted peridotites produced various enrichments of the rocks in Cpx and Gar and consequently in Al_2O_3, CaO, MREE, HREE, Y and Zr. FeO enrichment must be the last pulse of silicate metasomatose, as it influences the rocks independently of degree of their previous enrichments, and Gar's in FeO rich-rocks are often zoned. Thus, it should happen directly before incorporation of these xenoliths into kimberlite. The same Fe and incompatible elements rich liquid could be parental for megacryst association found in kimberlites. K-metasomatose could be a part of any metasomatic event described above. LILE enrichment was decoupled from other hardly incompatible elements by preferred incorporation of them into kelyphitic rims around the garnets.

The metasomatic process responsible for deformed peridotite formation and precipitation of megacrysts suite should not be widespread at the CM base, but rather local features only existing in CM below kimberlite fields and localized along metasomatic vein system. This conclusion arises from the independence of degree of deformation from estimated pressure and the fact of presence of undeformed rocks at pressure of 68 Kbar (Ionov et al, 2010). The deepest portion of CM is usually represented by deformed peridotites in nearly all kimberlites worldwide. It could be a result of preferable sampling of peridotites along metasomatic veins by kimberlite melt.

This work was supported by RFFI grant № 09-05-01179a

References

Agashev, A. M., Pokhilenko, N. P., Mal'kovets, V. G., Sobolev N.V. 2006. Sm-Nd isotopic system in garnet megacrysts from the Udachnaya kimberlite pipe (Yakutia) and petrogenesis of kimberlites. Dokl. Earth Sci. 407, 491

Agashev, A. M., Pokhilenko, N. P., Cherepanova, Yu. V., Golovin, A. V. 2010. Geochemical evolution of rocks at the base of the lithospheric mantle: Evidence from study of xenoliths of deformed peridotites from kimberlite of the Udachnaya pipe. Doklady Earth Sciences 432, 746-749.

Boyd, F.R., Pokhilenko, N.P., Pearson, D.G., et al. 1997. Composition of the Siberian cratonic mantle: evidence from Udachnaya peridotite xenoliths. Contribution to Mineralogy and Petrology 128, 228-246.

Burgess, S. R. & Harte, B. 2004. Tracing lithosphere evolution through the analysis of heterogeneous G9^G10 garnets in peridotite xenoliths, II: REE chemistry. Journal of Petrology 45, 609-633.

Ionov D., Doucet L., Ashchepkov I. 2010. Composition of the Lithospheric Mantle in the Siberian Craton: New Constraints from Fresh Peridotites in the Udachnaya-East Kimberlite. J. Petrology, 51, 2177-2210.

McDonough, W.F., Sun, S.-s., 1995. The composition of the Earth. Chemical Geology 120, 223-253.

O'Reilly, S.Y., Griffin, W.L., 2010. The continental lithosphere–asthenosphere boundary: Can we sample it? Lithos. doi:10.1016/j.lithos.2010.03.016

Pearson, D. G., Shirey, S. B., Carlson, R. W., Boyd, F. R., Pokhilenko, N. P. & Shimizu, N. 1995. Re-Os, Sm-Nd, and Rb-Sr isotope evidence for thick Archaean lithospheric mantle beneath the Siberian craton modified by multistage metasomatism. Geochimica et Cosmochimica Acta 59, 959-977.

Schmidberger, S. S., and Francis, D. 2001. Constrains on the trace elements composition of the Archean mantle root beneath Somerest Island, Arctic Canada. J. Petrology 42, 1095-1117.

Simon, N. S. C., Carlson, R. W., Pearson, D. G. & Davies, G. R. 2007. The origin and evolution of the Kaapvaal cratonic lithospheric mantle. Journal of Petrology 48, 589-625.

Stachel, T., Harris, J.W., 2008. The origin of cratonic diamonds — constraints from mineral inclusions. Ore Geology Reviews 34, 5–32.

Willbold, M., and Stracke, A. 2006. Trace element composition of mantle end-members: Implications for recycling of oceanic and upper and lower continental crust. Geochem. Geophys. Geosyst., (G3) v 7(4), doi:10.1029/2005GC001005.